Measurement errors in roentgen-stereophotogrammetric joint-motion analysis

J. Biomechanics Vol. 23, No. 3, pp. 259–269, 1990.
Printed in Great Britain

0021–9290/90 $3.00 + .00

MEASUREMENT ERRORS IN ROENTGEN-STEREOPHOTOGRAMMETRIC JOINT-MOTION ANALYSIS

A. DE LANGE,* R. HUISKES and J. M. G. KAUER

Biomechanics Section, Institute of Orthopaedics and Department of Anatomy and Embryology, University of Nijmegen, P.O. Box 9101, 6500 HB Nijmegen, The Netherlands

Abstract—In many biomechanical motion studies, kinematic parameters are estimated from position measurements on a number of landmarks. In the present investigation, dummy motion experiments are performed in order to study the error dependence of kinematic parameters on geometric factors (number of markers, isotropic vs anisotropic landmark distributions, landmark distribution size), on kinematic factors (rotation step magnitude, the presence of translational displacements, the distance of the landmarks' mean position to the rotation axis), and on anisotropically distributed measurement errors. The experimental results are compared with theoretical predictions of a previous error analysis assuming isotropic conditions for the measurement errors and for the spatial landmark distribution. In general, the experimental findings agree with the predictions of the error model. The kinematic parameters such as translations and rotations are well-determined by the model. In the helical motion description, the same applies for the finite rotation angle about and the finite shift along the helical axis. However, the direction and position of the helical axis are ill-determined. An anisotropic landmark distribution with relatively few markers located in the direction of the rotation axis will even aggravate the ill-posed nature of the finite helical axis estimation.

INTRODUCTION

Accurate measurements and descriptions of three-dimensional human-joint motions are increasingly important in Biomechanics. Popular measurement techniques are ultrasonic digitizers, cinephotogrammetry and roentgen-stereophotogrammetric analysis (RSA). These methods are discrete, in the sense that continuous rigid-body motions are approximated by step-wise, sequential displacements, and the kinematic parameters are estimated from sequential position measurements on a number of anatomical or artificial landmarks (Huiskes *et al.*, 1985a). Consequently, the accuracy of a description of the motions with kinematic parameters depends on landmark measurement errors. Woltring *et al.* (1985) presented an analytical error model in which this dependency is described. In the present paper the basic assumptions and the validity of the error model for applications to motion studies of human joints are investigated, using experimental methods.

Rigid-body motions are usually described by translation vectors, describing the spatial translation of a moving body-fixed coordinate system relative to an unmoving space-fixed system, and by rotation matrices, describing the sequential rotations (Euler angles) of the body-fixed system about its axes (e.g. Spoor and Veldpaus, 1980). A motion step of a moving bone relative to a fixed bone in a human joint can thus be quantified with six independent kinematic parameters, three translation components and three Euler rotations, once the positions of the space-fixed and body-fixed coordinate systems are uniquely defined before and after the motion step.

An alternative way of describing spatial rigid-body motions is by using the concept of helical or 'screw' axes (e.g. Woltring *et al.*, 1985). In this concept, the motion of the moving body, at any particular moment, is assumed to take place about and along a rotation axis, moving in space. For a particular motion step, this axis is a space-fixed entity, called the Finite Helical Axis (FHA: Woltring *et al.*, 1985), characterized by position and direction relative to the space-fixed coordinate system, and by a rotation and a translation of the moving body about and along its line of action. These characteristics can also be described by six independent (helical) parameters, discussed later. In the case of pure planar motion, the FHA degenerates to a point, the Finite Center of Rotation (FCR), for which error analyses were reported by Panjabi (1979), Soudan *et al.* (1979) and Panjabi *et al.* (1982a, b).

The error model of Woltring *et al.* (1985) predicts the standard deviations in the helical and the Euler parameters based on errors in the landmark position assessment, as represented by a standard deviation σ. The model is based on the assumption that these errors are relatively small, unbiased, uncorrelated, homogeneous and isotropic (equal standard deviations for all markers in all directions). It was also presumed that the landmark distribution is isotropic, i.e. that there are no preferential directions or planes in the marker distribution. The latter condition is fulfilled, for instance, if the markers are positioned at the vertices of a regular polyhedron, with or without a single marker at its center. Because of its importance for the present investigation, the model is briefly summarized here.

Received in final form 25 *August* 1989.
*Present Address: TNO Leather and Shoe Research Institute, Waalwijk, The Netherlands.
Reprints requests to Dr R. Huiskes.

Finite helical motion is described by the rotation (θ) about and the translation (t) along the helical axis, its direction (unit) vector (**n**), and the position vector (**s**) of a base point on the axis. For each of these variables, Woltring *et al.* (1985) derived analytical relations for their standard deviations, given the above conditions. For the case that the motion step is relatively small ($\theta \ll 1$ radian), it follows:

helical rotation: $$\sigma_\theta^2 = \frac{2\sigma^2}{m\rho^2} \quad (1)$$

helical direction: $$\sigma_{\mathbf{n}}^2 \simeq \frac{2\sigma_\theta^2}{\theta^2} \quad (2)$$

helical translation: $$\sigma_t^2 \simeq \frac{2\sigma^2}{m}\left(1+\frac{R^2}{\rho^2}\right) \quad (3)$$

helical position: $$\sigma_{\mathbf{s}}^2 \simeq \frac{4\sigma^2}{m\theta^2}\left(1+\frac{t^2}{\theta^2\rho^2}+\frac{R^2}{2\rho^2}\right) \quad (4)$$

where (Fig. 1):

σ = standard deviation of the landmark position errors,
m = number of markers,
ρ = the effective marker distribution radius, with $\rho^2 = 2/3\, r^2$, where r is the rms distance between the markers and their center of gravity,
θ = the rotation angle about the helical axis,
t = the translation distance along the helical axis,
p = the position vector of the midpoint P (Fig. 1) of the line between the landmarks' center of gravity, before the motion step (C_1) and after the motion step (C_2),
s = the position vector of the projection of **p** onto the helical axis,
n = the unit direction vector of the helical axis,
R = The distance of the landmarks' center of gravity to the FHA, where $R = |\mathbf{s}-\mathbf{p}|/\cos(\frac{1}{2}\theta)$.

The Eulerian motion description uses rotations (θ_i, $i=1, 2, 3$) about and translations (d_i, $i=1, 2, 3$) along Cartesian coordinate axes. Assuming small rotations ($|\theta_i| \ll 1$ radian), and taking the origin of the body-fixed coordinate system in the center of gravity of the landmark distribution, Woltring *et al.* (1985) found for the translational and rotational standard deviations:

translation $$\sigma_{d_i}^2 = \frac{2\sigma^2}{m} \quad (5)$$

rotation $$\sigma_{\theta_i}^2 = \frac{2\sigma^2}{m\rho^2} \quad (6)$$

where:

θ_i = the rotation angle about the ith Cartesian coordinate axis, $i=1, 2, 3$,
d_i = the translation component along the ith Cartesian coordinate axis; $i=1, 2, 3$.

It is obvious from these expressions that the accuracy of the kinematical parameters depends, apart from measurement errors in the landmark position data (σ), on geometrical parameters as well, such as the number and the distribution characteristics of the markers. In addition, the helical axis position and direction errors also depend on the magnitude of the motion step (θ and/or t).

In a numerical analysis, using 'Monto Carlo' simulation, Spoor (1984) validated the isotropic error model of Woltring *et al.* (1985), assuming the same conditions. However, the requirements for isotropy in the measurement errors and in the landmark distribution can rarely be met in practice. For example, when using the RSA technique, the measured landmark coordinates towards the roentgen foci are more prone to error than the other coordinates, depending on the experimental configuration. In addition, the landmarks will usually not be distributed isotropically since, in general, they are inserted into the bones in an arbitrary fashion.

The purpose of the present study was to investigate the effects of non-isotropic conditions on the error model, using RSA techniques in a dummy experiment, simulating wrist-joint (de Lange *et al.*, 1985) and knee-joint (Blankevoort *et al.*, 1988) motion studies.

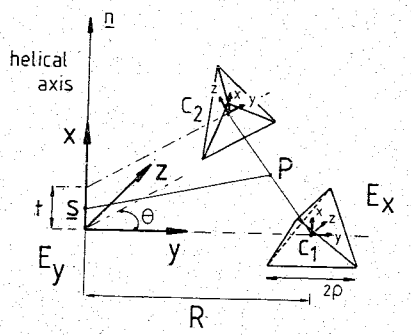

Fig. 1. Fixed coordinate system E_y in which a rigid body (regular tetrahydron) with a body-fixed coordinate system E_x moves from position 1 to position 2 along a finite helical axis with position **s** and direction **n**. C_1 and C_2 are the mean positions of the landmarks in position 1 and 2, respectively. C_1 and C_2 are both at a distance R from the helical axis.

METHODS AND MATERIAL

The mechanism, constructed for the tests, contains two rigid bodies (glass cubes) applied with tantalum roentgen markers. The cubes can move relative to each other (Fig. 2). The first cube can rotate about and shift along axis 1, and together with the frame containing axis 1, rotate about axis 2. The second cube can only rotate about axis 3. In the present investigation, however, the second cube was always considered the space-fixed body and kept stationary, whereas the first cube was only rotated about and shifted along axis 1. The rotational and translational motion steps could be prescribed reasonably accurately relative to a protractor, mounted to the test frame (Fig. 2), and relative to equidistant markers on the axis 1, respectively.

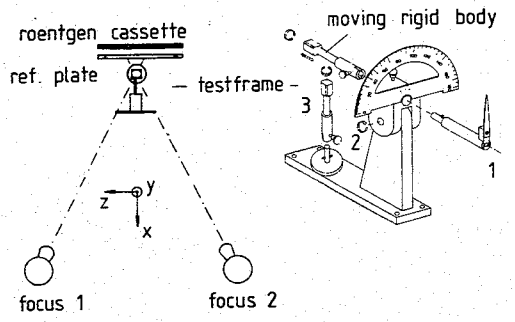

Fig. 2. The roentgen-stereophotogrammetric set-up (left) with the test frame (right). Rotations can be prescribed about three fixed axes, indicated by the numbers 1, 2 and 3. Along axis 1, translations can be prescribed as well. During the experiments the rotation axis 1 (x-axis) was directly perpendicular to the roentgen cassette.

The rigid-body motions were determined using a roentgen-stereophotogrammetric analysis (RSA) technique described earlier (Selvik, 1974; Huiskes *et al.*, 1985a; de Lange *et al.*, 1985; Blankevoort *et al.*, 1988).

The test frame was positioned in front of a reference plate and a roentgenfilm cassette, with its axis 1 (x-axis) perpendicular to the plate (Fig. 2). After each motion step, double roentgen exposures were made, using two roentgen foci, thereby projecting the markers of the reference plate and the tantalum landmarks contained in the glass cubes. The two cubes in the test frame were approximately 0.1 m from the cassette, near the mid-perpendicular from the baseline between the two foci onto the cassette (Fig. 2). The two roentgen foci were about 1.0 m apart and 1.2 m from the cassette. Prior to the start of the experiments, the relative positions of the roentgen foci, the film cassette and the reference plate were determined in a laboratory coordinate system which was defined by markers in a calibration cage (de Lange *et al.*, 1985).

After the experiments, the photographs were developed and manually digitized on a two-dimensional coordinate digitizer (ARISTOMAT® 104 M two dimensional mechanical digitizer) with an experimentally verified pellet image digitization repeatability between 10 and 20 μm (standard deviation per image coordinate; Huiskes *et al.*, 1985b). Using the software package of Selvik (1974), the individual landmark coordinates were reconstructed via photogrammetrical triangulation for stereophotographs individually, and a rigid-body model was fitted to corresponding sets of landmarks of the fixed and moving rigid body between subsequent positions. In these steps, redundant data were available and optimization occurred in terms of an unweighted least-squares criterion (Selvik, 1974).

For each experiment, Cartesian coordinate systems were defined on the two cubes, with the coordinate axes in the reference position parallel to those of the laboratory coordinate system with origins coinciding with the landmark's mean positions (or centers of gravity of the cubes). For each motion step, the relative motion of the moving cube with respect to the fixed cube was quantified in terms of three rotations about the three coordinate axes in the moving body (sequence 1, x-axis; 2, y-axis; 3, z-axis) and of the three translations of the moving body's origin along the axes of the coordinate system in the fixed body (Selvik, 1974). On the basis of these completed data, the finite helical axis (FHA) parameters were determined using Rodriques' formula (Selvik, 1974), which is similar to the one used in the analysis of Woltring *et al.* (1985), as described by Spoor and Veldpaus (1980).

For this RSA measurement configuration it was shown previously (Woltring *et al.*, 1985) that the errors in the reconstructed landmark coordinates are anisotropic, i.e. the errors in the direction towards the foci are larger than those in the other directions, parallel to the roentgen cassette. Hence, throughout the experiments, anisotropic measurement errors in the marker coordinates were present.

The experimental procedure, whereby several geometric and kinematic conditions were varied, is outlined in Table 1.

In order to study effects of the landmark distribution radius, glass-cube pairs were fabricated in two different sizes. The smallest pair is similar in size to the carpal bones in the wrist joint and the largest pair similar to the knee-joint bones. These cubes were applied with 8 tantalum pellets of 0.8 mm diameter at the vertices (see distribution 1 in Fig. 3). In the small-sized pair, the landmarks were placed 10 mm from each other; in the other pair, the distances were 30 mm. Thus, two pairs of landmark configurations, both isotropic, were available, of which the rms distance of the landmarks to the centers of gravity were 8.66 mm and 25.98 mm respectively. Hence, the effective marker distribution radii were 7.07 mm and 21.21 mm.

Of the 8 markers, 4 markers were chosen for the normal data evaluation, while maintaining the isotropic distribution condition (see distribution 2^a in Fig. 3). To study the effect of the number of landmarks, the results of these experiments were compared to an evaluation with all the 8 markers (distribution 1 in Fig. 3).

To study the influence of anisotropic landmark configurations, alternative sets of 4 markers were chosen (distribution $2^{b,c,d}$ in Fig. 3), resulting in three anisotropic landmark configurations, of which one has its center of gravity on the helical axis (distribution 2^b) and the others 2.5 mm (distribution 2^c) and 5 mm (distribution 2^d) from the helical axis.

As indicated by the error model, the distance of the landmark distribution center with respect to the helical axis is an important parameter in the accuracy of the helical position and translation estimates. To study its effect, the landmarks' center of gravity of the moving small test cube was placed on the helical axis in most experiments, and to a distance of 120 mm in two others.

To study the effects of measurement errors on the

Table 1. Experimental series and values for the kinematic and geometric variables used. The underlined values are variations relative to the reference values

	Kinematic variables			Geometric variables		
Series number	Cube size	Rotation θ (deg)	Translation t (mm)	Distribution ρ (mm)	Number of markers m	Distance midpoint to helical axis R (mm)
$T1$	small	1	0	7.07	4	0
$T1'$	small	1	0	7.07	8	0
Q	large	1	0	7.07	4	0
$T2$	small	5	0	7.07	4	0
$T3$	small	10	0	7.07	4	0
$T4$	small	15	0	7.07	4	0
$T5$	small	20	0	7.07	4	0
$T6$	small	1	1	7.07	4	0
$T7$	small	1	2	7.07	4	0
$T8$	small	1	0	21.21	4	0
$T9$	small	1	0	7.07	4	120
$T10$	small	1	1	7.07	4	120

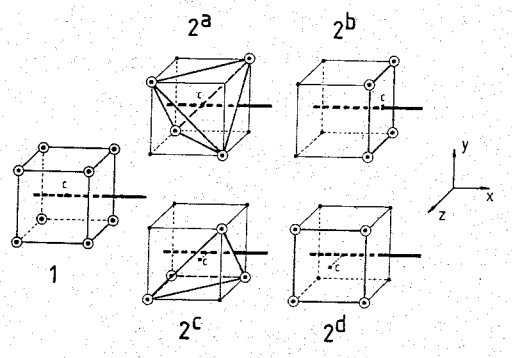

Fig. 3. The marker distribution used, of which two are isotropic (numbers 1 and 2^a) and three anisotropic (2^{b-d}). Distribution number 1 consists of 8 markers at the vertices of the cube, the others have 4 markers.

kinematic parameters, a different set of film cassettes was used in one experiment. It was known that these produced irregular bending of films resulting in relatively large reconstruction errors. This particular experiment will be denoted by Q, whereas all other experiments are denoted by T (Table 1).

In total, 11 different sets of experiments were performed (see Table 1). In each set, a displacement of the 'moving' test cube was executed 5 times (one step and four repetitions). During all the experiments, the moving rigid body was rotated about a fixed helical axis normal to the roentgen cassette. This was done because in most joint-motion studies in which the RSA method is used, (de Lange *et al.*, 1985; Blankevoort *et al.*, 1988) the principal motions usually occur in planes parallel to the roentgen cassette. Hence, the helical axes are usually directed more-or-less perpendicular to the image planes.

Data evaluation

To evaluate the measurement errors in the landmark coordinates in each experiment ($k=5$ motion steps each), the 10 sets of marker coordinates of an arbitrarily chosen marker in the fixed rigid body were used. The mean value of the coordinate in the x-direction, with its standard deviations (σ_x) was calculated from

$$\bar{x}=\frac{1}{n}\sum_{i=1}^{n} x_i \tag{7}$$

$$\sigma_x=\left[\frac{1}{n-1}\sum_{i=1}^{n}(x_i-\bar{x})^2\right]^{1/2} \tag{8}$$

where n is the number of positions (10 in this case) and x_i the coordinate of the marker in position i of the test cube; $\bar{y}$, σ_y, $\bar{z}$, and σ_z were estimated in a similar fashion.

For each kinematic variable, a value was obtained for each of the 5 motion steps in each experiment. To determine quality expressions for these variables, different methods were used, depending on whether their values were *a priori* known or not.

In the case of a rotation without helical shift, i.e. $t=0$ and $d_i=0$, the standard deviations in the estimated translation components were calculated according to:

$$\sigma_t=\left[\frac{1}{k}\sum_{j=1}^{k}(t_j)^2\right]^{1/2} \tag{9}$$

where $k(=5)$ is the number of displacement steps; d_i $(i=1, 2, 3)$ were determined accordingly.

In the case that translations were prescribed but not known exactly (i.e. $t\approx 1$ mm or $t\approx 2$ mm) the standard deviations in the translation components were calculated according to:

$$\sigma_t=\left[\frac{1}{k-1}\sum_{j=1}^{k}(t_j-\bar{t})^2\right]^{1/2} \tag{10}$$

$$\bar{t}=\frac{1}{k}\sum_{j=1}^{k} t_j. \tag{11}$$

Since the precise magnitudes of the prescribed rotations were also unknown *a priori*, the expressions (10) and (11) were also used in a similar way to calculate the standard deviations in the rotation components (θ and θ_i; $i=1, 2, 3$).

In the experiments, the rotation axes were fixed. However, their precise locations were not *a priori* known relative to the space-fixed coordinate system. To provide an indication of the precision of the FHA estimation procedure, the dispersion of the FHAs were calculated with respect to a Mean Helical Axis (MHA: Woltring, 1990). The MHA for the FHAs found for the 5 motion steps in each experiment was determined in two steps. First a mean rotation 'pivot' of the FHAs was calculated. This rms value is denoted $X_{\mathbf{n}}$ and is considered as an estimate for the standard deviation in the helical position vector ($\sigma_{\mathbf{s}}$). Subsequently, an average direction vector was defined through this pivot by minimizing the rms values of the sines of the angles between the MHA and the FHAs. The angular dispersion is defined as the arcsine of this rms value, which is denoted as $D_{\mathbf{s}}$ and is considered as an estimate of the standard deviation in the helical direction vector ($\sigma_{\mathbf{n}}$).

In order to test the validity of the analytical error model of Woltring *et al.* (1985), corresponding values of the geometric and kinematic quantities as applied in the different experiments were used for error calculations with the formulas. In the case of modeling the *T*-experiments, a standard deviation of the landmark measurement errors of 20 μm was assumed, whereas in the case of the *Q*-experiment a value of 80 μm was taken. The choice of both values was based on sets of (anisotropic) measurement error values found experimentally (Table 2).

Table 2. Measurement errors (standard deviations) in the *x*-, *y*- and *z*-coordinates of the reconstructed tantalum pellets in each experiment

Series number	Precision		
	x (μm)	*y* (μm)	*z* (μm)
*T*1	20	10	10
Q	116	21	43
*T*2	23	15	12
*T*3	21	12	12
*T*4	16	8	9
*T*5	23	15	11
*T*6	19	10	10
*T*7	21	11	10
*T*8	33	16	14
*T*9	17	11	8
*T*10	22	12	11

RESULTS

In Table 2 the standard deviations in the measurement errors of the landmark coordinates are shown. Evidently, the measurement errors in the *T*-experiments are lower than those in the *Q*-experiment and in both cases the *x*-coordinate perpendicular to the roentgen cassette in the direction towards the foci is subject to the highest error.

The further results were divided in two parts. In one part the marker distributions are isotropic (distributions 1 and 2^a in Fig. 3). The other part contains data relative to the anisotropic landmark distributions (distribution 2^a vs $2^{b,c,d}$ in Fig. 3).

Isotropic marker distributions

The effects of the marker reduction from 8 to 4 on the kinematic parameters (experiment *T*1) are shown in Table 3. Decreasing the number of markers results in an increase of the standard deviations of the kinematic parameters, in accordance with the error model predictions. Some differences are found when comparing the (anisotropic) experimental results with the (isotropic) model predictions. Apparently, the enlarged measurement errors in the direction of the *x*-axis (parallel to the rotation axis) have the most influence on the errors in the translations d_1 and t along the *x*-axis, and in the rotations θ_2 and θ_3 about the *y*- and *z*-axes respectively. Furthermore, the experimental errors in the rotations θ_1 and θ, both about the *x*-axis, are much smaller than predicted by the model. The experimental errors in the helical axis position (**s** and **n**) are similar to the theoretical ones.

The effects of the rotation step magnitude on the Euler kinematic parameters are presented in Table 4. According to the error model [equations (5) and (6)], these errors are independent from the rotation-step magnitude, and indeed, no clear relation pattern is

Table 3. Standard deviations resulting from the T_1 experiment ($\theta = 1°$, $t = 0$ mm, $R = 0$ mm, $\rho = 7.07$ mm) and the error model, for two different amounts of markers, both isotropically distributed

	Errors with respect to									
	θ_1 (deg)	θ_2 (deg)	θ_3 (deg)	d_1 (μm)	d_2 (μm)	d_3 (μm)	θ (deg)	t (μm)	**s** (μm)	**n** (deg)
Experiment										
$m=8$	0.03	0.06	0.07	21	16	15	0.03	21	1048	5.06
$m=4$	0.04	0.09	0.10	27	20	20	0.04	26	1221	6.02
Model										
$m=8$	0.08	0.08	0.08	10	10	10	0.08	10	810	6.57
$m=4$	0.11	0.11	0.11	14	14	14	0.11	14	1145	9.29

Table 4. Standard deviations calculated for five experiments (T_1–T_5) in which only the rotation-step magnitude is varied ($m = 4$, $t = 0$ mm, $R = 0$ mm, $\rho = 7.07$ mm). In all the five cases, the error model predicts equal standard deviations in the three rotational and three translational components

	Errors with respect to					
	θ_1 (deg)	θ_2 (deg)	θ_3 (deg)	d_1 (μm)	d_2 (μm)	d_3 (μm)
Experiment						
$\theta = 1°$	0.04	0.09	0.10	27	20	20
$\theta = 5°$	0.04	0.08	0.06	31	19	16
$\theta = 10°$	0.03	0.07	0.07	21	11	15
$\theta = 15°$	0.07	0.09	0.09	14	20	14
$\theta = 20°$	0.04	0.12	0.09	34	19	40
Model						
$\theta = 20° - 1°$	0.11	0.11	0.11	14	14	14

found in the experimental results here. The model underestimates the translation error in d_1, along the x-axis in particular. Figure 4 shows the effects of the rotation-step magnitude with respect to the helical axis parameters. The helical position and direction errors increase almost linearly with the inverse rotation step magnitude. The experimental helical position errors are higher and the helical direction errors are lower than predicted by the model. The error in the rotation magnitude (θ) is considerably overestimated by the model, approximately by a factor of 3, as was also found for the Euler rotation about the x-axis (θ_1, Table 3). The helical translation error is about 50% underestimated by the model; again the same tendency was found in the translation along the x-axis (d_1, Table 4). The helical rotation and translation errors varied between 0.04–0.07 degrees and 14–34 μm, respectively, and are hardly susceptible to reductions of the rotation step magnitude. These tendencies correspond with the error model predictions.

The occurrence of a translation t in the rigid-body motion would, according to the error model, only affect the helical position error. This is confirmed by the experimental results (Table 5), although the experimental effects are less pronounced than the model predicts.

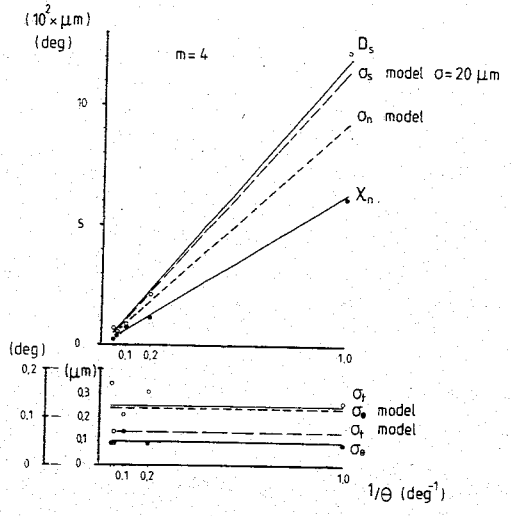

Fig. 4. The helical parameter errors as functions of the inverse value of the rotation-step magnitude, as found in the experiments (T_{1-5}) and as predicted by the error model (isotropic landmark distribution with $m = 4$ markers). The top graph shows the errors relative to the axis position (**s**) and direction (**n**), as determined in the model (σ_s, σ_n) and estimated from the experiments (D_s, X_n). The bottom graph shows the comparison for the errors relative to the rotation about (σ_θ) and the translation along (σ_t) the helical axis. All angular dimensions are in degrees; all length dimensions are in μm/100.

Enlarging the radius of the marker distribution by a factor of 3 resulted in an increase of the translation errors with respect to d_1 and t along the x-axis (Table 6). The translation error of d_2 along the y-axis decreased. However, according to the model, the translation errors should not be influenced by the distribution radius of the markers. The experimental effects may be explained by the differences in the measurement errors of the marker position in the different experiments (Table 2). The errors in the rotations are predicted to decrease when increasing the distribution radius. Experimentally, this is only found for θ_2 and θ_3 while both the rotation θ_1 and θ remained practically unchanged, which may again be explained by the larger marker position errors in the

Table 5. Standard deviations, resulting from three different prescribed translations t ($m = 4$, $\theta = 1°$, $R = 0$ mm, $\rho = 7.07$ mm)

	Errors with respect to									
	θ_1 (deg)	θ_2 (deg)	θ_3 (deg)	d_1 (μm)	d_2 (μm)	d_3 (μm)	θ (deg)	t (μm)	**s** (μm)	**n** (deg)
Experiment										
$t = 0$ mm	0.04	0.09	0.10	27	20	20	0.04	26	1221	6.02
$t = 1$ mm	0.06	0.06	0.08	19	17	9	0.06	21	5843	5.38
$t = 2$ mm	0.07	0.10	0.06	24	20	28	0.07	35	12596	6.04
Model										
$t = 0$ mm	0.11	0.11	0.11	14	14	14	0.11	14	1145	9.29
$t = 1$ mm	0.11	0.11	0.11	14	14	14	0.11	14	9355	9.29
$t = 2$ mm	0.11	0.11	0.11	14	14	14	0.11	14	18522	9.29

Table 6. Standard deviations, calculated for two different radii of the marker distribution ($m = 4$, $\theta = 1°$, $t = 0$ mm, $R = 0$ mm)

	Errors with respect to									
	θ_1 (deg)	θ_2 (deg)	θ_3 (deg)	d_1 (μm)	d_2 (μm)	d_3 (μm)	θ (deg)	t (μm)	**s** (μm)	**n** (deg)
Experiment										
$\rho = 7.07$ mm	0.04	0.09	0.10	27	20	20	0.04	25	1221	6.02
$\rho = 21.21$ mm	0.03	0.03	0.03	50	10	22	0.03	50	1175	2.20
Model										
$\rho = 7.07$ mm	0.11	0.11	0.11	14	14	14	0.11	14	1145	9.29
$\rho = 21.21$ mm	0.04	0.04	0.04	14	14	14	0.04	14	1145	3.07

Table 7. Standard deviations, calculated for three combinations of translations and distances of the landmarks' mean position to the rotation axis ($m = 4$, $\theta = 1°$, $\rho = 7.07$ mm)

	Errors with respect to										
	θ_1 (deg)	θ_2 (deg)	θ_3 (deg)	d_1 (μm)	d_2 (μm)	d_3 (μm)	θ (deg)	t (μm)	**s** (μm)	**n** (deg)	
Experiment											
$t=0$ $R=0$	0.04	0.09	0.10	27	20	20	0.04	26	1221	6.02	Ref.
$t=0$ $R=120$	0.05	0.07	0.06	36	14	11	0.05	139	4158	4.78	Case 1
$t=1$ $R=120$	0.05	0.08	0.06	16	18	15	0.05	169	6081	5.10	Case 2
Model											
$t=0$ $R=0$	0.11	0.11	0.11	14	14	14	0.11	14	1145	9.29	Ref.
$t=0$ $R=120$	0.11	0.11	0.11	14	14	14	0.11	240	13798	9.29	Case 1
$t=1$ $R=120$	0.11	0.11	0.11	14	14	14	0.11	240	16632	9.29	Case 2

Table 8. Standard deviations, calculated for the error model and obtained from the experiment, for two different sets of landmark measurement errors ($m = 4$, $\theta = 1°$, $t = 0$ mm, $R = 0$ mm, $\rho = 7.07$ mm)

	Errors with respect to									
	θ_1 (deg)	θ_2 (deg)	θ_3 (deg)	d_1 (μm)	d_2 (μm)	d_3 (μm)	θ (deg)	t (μm)	**s** (μm)	**n** (deg)
Experiment										
$T1$	0.04	0.09	0.10	27	20	20	0.04	26	1221	6.02
Q	0.05	0.07	0.20	120	22	28	0.05	117	2076	10.36
Model										
$\sigma = 20$ μm	0.11	0.11	0.11	14	14	14	0.11	14	1145	9.29
$\sigma = 80$ μm	0.46	0.46	0.46	57	57	57	0.46	57	4584	37.14

experiment T_8 (Table 2). The decrease in the helical direction error, predicted in the model as an effect of an increase of the marker-distribution radius, is confirmed by the experimental results.

In Table 7, the effects on the kinematic parameters are shown when, in the first case, the moving rigid body is displaced 120 mm from the rotation axis and is rotated about this axis and, in the second case, when a translation of 1 mm along the rotation axis is added to this rotation. In both cases, compared to the reference case ($R = 0$, $t = 0$ mm, $\rho = 7.07$ mm), only an increase of the helical translation and position errors is to be expected from the model. These effects are also observed in the experiments.

An increase in the errors of the marker coordinates in the x- y- and z-axis directions with factors 5, 2 and 4, respectively (see Table 2), produced an error increase in the translations t and d_1 by a factor of 5, whereas in the other parameters error changes occurred to factors of 0.8–2.0 (Table 8). Due to the fact that the error model presumes isotropic landmark position errors, these effects are only partly accounted for in the predictions.

Isotropic vs anisotropic marker distributions

The effects on the error values of the Euler motion parameters, when changing the marker distribution from isotropic to anisotropic, are shown in Table 9 (compare Fig. 3). Variations in the error values of the translations were noticed. However, definite tendencies were not found. The errors in the rotations θ_2 and θ_3 are obviously increased by the distribution number 2^b, in which the markers are positioned in a plane perpendicular to the rotation axis. The errors in

the rotation θ_1 tend to increase when using any of the anisotropic marker distributions.

When varying the kinematic and geometric parameters, similar tendencies in the errors in the Euler kinematic parameters are observed for the anisotropic landmark distributions as previously described for the isotropic distributions.

Concerning the anisotropic landmark effects on the helical parameters, the errors in the helical rotations varied between 0.02 and 0.07 degrees in all cases; definite tendencies could not be found. Overall, the error in this parameter remained virtually unchanged. For the helical translation, direction and position, the effects of anisotropic marker distributions are shown graphically in Figs 5–8. In these figures it can be seen in the reference case ($\theta = 1°$, $t = 0$, $R = 0$, $\rho = 7.07$ mm) that only the error in the helical direction is significantly increased by the marker distribution 2^b. The qualitative effects of the parametric variations (T_2–T_{11}) with the anisotropic landmark distributions were similar to those found for the isotropic distributions. In the cases that significant quantitative differ-

Table 9. Standard deviations, calculated for one isotropic (2^a) and three anisotropic marker distributions (2^{b-d}, see Fig. 3) ($m = 4$, $t = 0$ mm, $R = 0$ mm, $\rho = 7.07$ mm)

	Errors with respect to					
	θ_1 (deg)	θ_2 (deg)	θ_3 (deg)	d_1 (μm)	d_2 (μm)	d_3 (μm)
Experiment distr. no.						
2^a	0.04	0.09	0.10	27	20	20
2^b	0.05	0.12	0.19	24	17	14
2^c	0.06	0.02	0.09	25	20	13
2^d	0.07	0.05	0.10	21	18	10

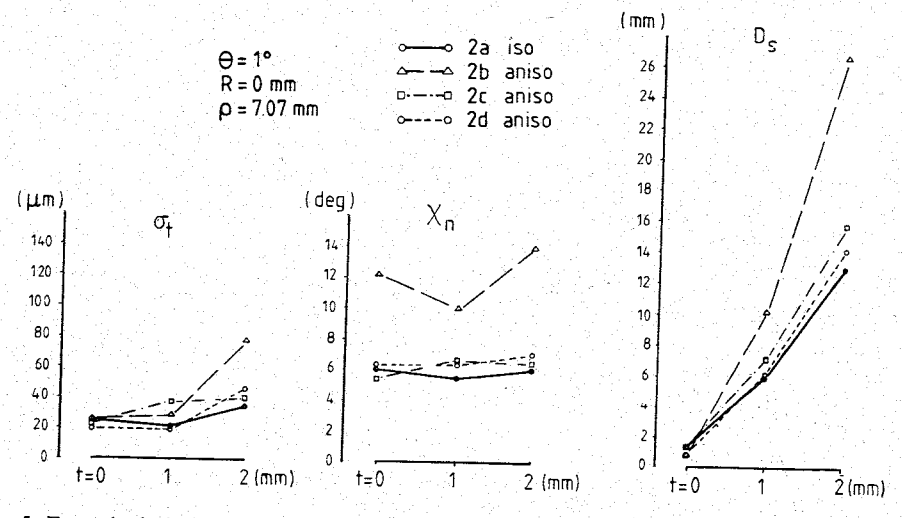

Fig. 5. Errors in the helical translation (σ_t), direction (X_n) and position (D_s) as functions of the helical shift t, obtained for four different marker distributions (see Fig. 3: 2^{a-d}).

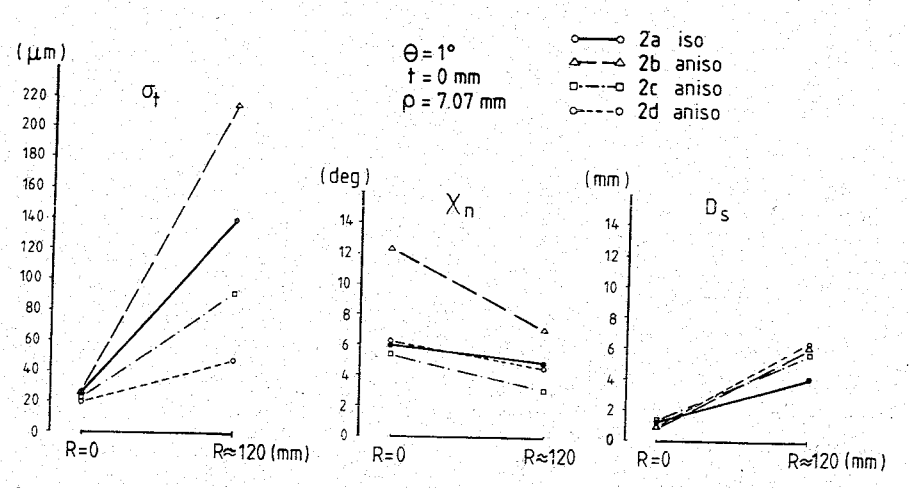

Fig. 6. Errors in the helical translation (σ_t), direction (X_n) and position (D_s) as functions of the midpoint distance R to the helical axis, for four different marker distributions (see Fig. 3: 2^{a-d}).

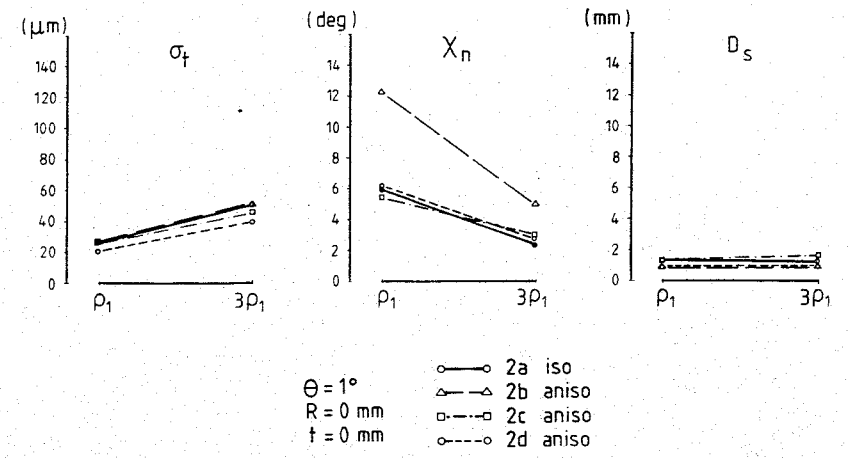

Fig. 7. Errors in the helical translation (σ_t), direction (X_n) and position (D_s) as functions of the effective landmark distribution radius ρ, for four different marker distributions (see Fig. 3: 2^{a-d}).

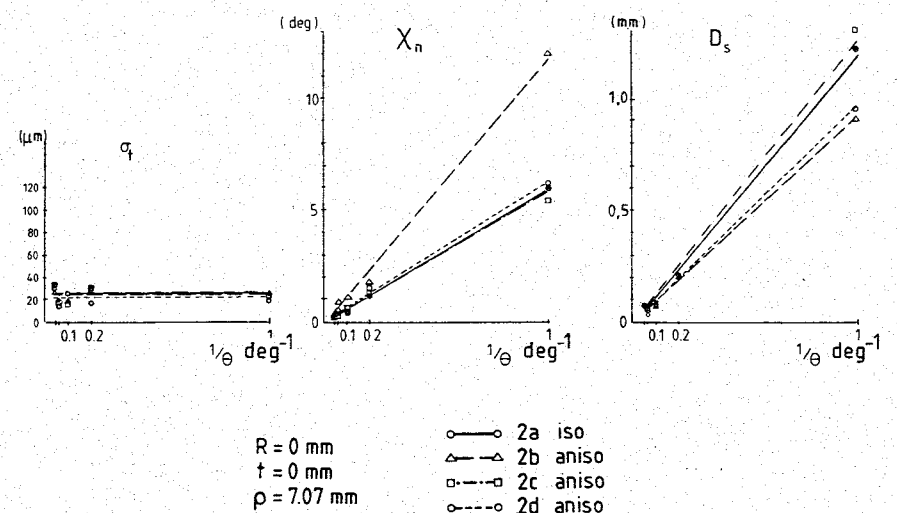

Fig. 8. Errors in the helical translation (σ_t), direction (X_n) and position (D_s) as functions of the inverse value of the rotation magnitude θ^{-1}, for four different marker distributions (see Fig. 3: 2^{a-d}).

ences occurred, these were most pronounced for the distribution 2^b (Figs. 5–8).

DISCUSSION

In order to investigate the error dependence in kinematic parameters a dummy motion experiment was performed in which kinematic and geometric quantities were varied, and different isotropic and anisotropic marker distributions were used. The experimental results were compared with predictions of the error model of Woltring *et al.* (1985), in which isotropic conditions with respect to measurement errors and landmark distributions are presumed. It appears from the present study that, even for anisotropic measurement errors and landmark distributions, the isotropic error model maintains its approximate predictive value.

The Euler rotation angles about and the translations along the coordinate axes are not very sensitive for measurement errors. The same is true for the rotation angle about the helical axis and for the helical translation. The direction and the position of the helical axis, however, are very sensitive to landmark measurement errors, particularly in cases of small rotations, large distances to the mid-point of the landmark distribution, or small landmark distribution sizes.

In a qualitative sense, the error dependence in the kinematic parameters experimentally found is in agreement with the model predictions. For example, in terms of helical motion, the errors in the helical position and direction are inversely proportional to the rotation magnitude, and the helical translation and rotation errors are not influenced by the rotation magnitude (see Fig. 4).

In a quantitative sense, differences occur which of course may be related, in the first instance, to the difference between the measurement errors in the

experiment and those assumed in the model. The accuracies in the rotations θ_2 and θ_3 around the y-axis and the z-axis respectively, those in the translation d_1 along the x-axis, and those in both the helical translation t and position **s**, are predominantly affected by errors in the x-direction, which are relatively large in the experiment. Regarding the helical position error, this can be directly concluded from the error model: the residual difference between the measurement errors in the x-direction and those in the other two directions can be interpreted as a shift along the x-axis or the helical axis. According to the error model, such a shift contributes to the helical position error.

The accuracies in the translations d_2 and d_3 along the y-axis and z-axis, respectively, and in the rotation θ_1 about the x-axis will be mostly influenced by the measurement errors in the y- and z-directions. Considering the relationship between the helical rotation and direction on the one hand, and the three rotations about the coordinate axes, on the other, it is evident that the helical rotation error will be largely affected by the error in the rotation θ_1, which is mostly influenced by the measurement errors in the y- and z-coordinates of the markers. The error in the helical direction **n** is largely affected by the errors in the rotations θ_2 and θ_3, which on their turn are predominantly affected by the measurement errors in the x-direction.

The experimental errors in the rotation θ_1 and the helical rotation θ are found to be much less than those predicted by the model. These differences are explained by the fact that both kinematic parameters are, as previously described, mostly influenced by the errors in the y- and z-coordinates while in the model a measurement error value is assumed which is based on the experimentally obtained errors in the x-direction.

The experimental errors in the helical direction **n** and helical translation t, however, are found to be substantially different from the model predictions, while 'similar' values are expected since both kinematic parameters are predominantly influenced by measurement errors in the x-direction. A possible explanation is the presence of systematic errors in the marker reconstruction caused by (small) bending effects of the roentgen image planes in the cassettes. These systematic errors in the landmark coordinates will not be equal in all reconstructed positions of the rigid bodies, since on the one hand the bending differs in each cassette and, on the other, the cassettes were randomly used in the experiment. As a consequence, the stochastic errors in the marker coordinates are lower than assumed in the model, while variable systematic errors are present in each axis direction. These systematic errors may be interpreted as (small) translations of the moving rigid body along the axis. According to the error model, the accuracy in the helical direction (**n**) will not be influenced by such a translation. Hence, the stochastic errors remain and the experimental errors in the helical direction are found to be lower than predicted by the model. On the other hand, the systematic errors will certainly influence the helical translation t (and translations d_2 and d_3) apparently resulting in higher error values in the experiments than in the model.

The existence of systematic errors might also explain the noted differences between model and experiment with respect to errors in the helical position (**s**). In cases where (prescribed) translations are present ($t \approx 1$ mm and $t \approx 2$ mm; T_{6-7} experiments) or the landmarks' center of gravity is at a distance from the axis ($R = 120$ mm; T_{9-10} experiments), the helical position error caused by systematic errors (small t values) is negligible compared to the error caused by the quantities in equation (4). Hence, in these experimental cases, the helical position error depends mostly on the stochastic errors and is found to be lower compared to model values. In the other experimental cases ($t = 0$ mm, $R = 0$ mm; T_{1-5}, T_8 experiments), the systematic errors contribute as additional translations to the helical position error, and equal or larger error values for this kinematic parameter are found than in the model.

Evidently, the isotropic error model may serve as a useful tool in the preparation of kinematical experiments and in the evaluation of kinematic results. The application of the model is not limited to situations in which isotropic marker distributions are used. In the present investigation the effects of three different anisotropic marker distributions were studied and it appeared that only in the case of positioning the landmarks in one plane perpendicular to the rotation axis (distribution 2^b), the errors in (most) kinematic parameters increased considerably compared to corresponding error values in the isotropic distribution case. In the other two anisotropic marker distribution cases (2^c and 2^d) similar results were obtained. In addition, in all the three cases the tendencies in the error dependence of the kinematic parameters predicted by the error model were evident.

As a consequence, it is suggested that in three-dimensional kinematic experiments the landmarks in the moving rigid body (or bodies) should be distributed, if possible, in the direction parallel to that of the helical axis. In addition, as also follows directly from the error model, the landmark distribution should be sufficiently large and its center of gravity close to the anticipated helical axis.

From the model and the present experimental results, it follows that when decreasing the (rotation) step magnitude or sampling interval in order to obtain a closer description of the continuous rigid-body motion, the finite helical axis may become an inaccurate model for the instantaneous helical axis. As indicated previously by Woltring and Huiskes (1985), when estimating discrete samples of the instantaneous helical axis, the use of a smoothing procedure is to be preferred in order to reduce the measurement error.

Acknowledgements—The authors gratefully acknowledge the assistance of P. van den Braak, I. de Bruin (Department of

Anatomy and Embryology, University of Nijmegen); H. Peeters, J. de Vocht (Institute of Orthopaedics, Biomechanics Section, University of Nijmegen); and H. J. Woltring (Philips Medical Systems, Best, The Netherlands).

REFERENCES

Blankevoort, L., Huiskes, R. and Lange, A. de (1988) The envelope of passive knee joint motion. *J. Biomechanics* **21,** 705–720.

Huiskes, R., Dijk, R. van, Lange, A. de, Woltring, H. J. and Rens, Th. J. G. van (1985a) Kinematics of the human knee joint. In: *Biomechanics of Normal and Pathological Human Articulating Joints* (Edited by Berme, N., Engin, A. and Correia da Silva, L), pp. 165–187. Martinus Nijhoff, The Hague.

Huiskes, R., Kremers J., Lange, A. de, Woltring, H. J., Selvik, G. and Rens, Th. J. G. van (1985b) Analytical stereophotogrammetric determination of three-dimensional knee-joint geometry. *J. Biomechanics* **18,** 559–570.

Lange, A. de, Kauer, J. M. G. and Huiskes, R. (1985) Kinematic behavior of the human wrist joint: A roentgen-stereophotogrammetric analysis. *J. orthop. Res.* **3,** 56–64.

Panjabi, M. M. (1979) Centres and angles of rotation of body joints: a study of errors and optimization. *J. Biomechanics* **12,** 911–920.

Panjabi, M. M., Goel, V. K. and Walter, S. D. (1982a) Errors in kinematic parameters of a planar joint: guidelines for optimal experimental design. *J. Biomechanics* **15,** 537–544.

Panjabi, M. M., Goel, V. K., Walter, S. D. and Schick, S. (1982b) Errors in the center and angle of rotation of a joint: an experimental study. *J. biomech. Engng* **104,** 232–237.

Selvik, G. (1974) A Roentgenstereophotogrammetric method for the study of the kinematics of the skeletal system. Thesis, University of Lund, Sweden.

Soudan, K., Audekercke, R. van and Martens, M. (1979) Methods, difficulties and inaccuracies in the study of human joint kinematics and patho-kinematics by the instant axis concept. Example: the knee joint. *J. Biomechanics* **12,** 27–33.

Spoor, C. W. (1984) Explanation, verification and application of helical axis error propagation formulas. *Hum. Mov. Sci.* **3,** 95–117.

Spoor, C. W. and Veldpaus, F. E. (1980) Rigid body motion calculated from spatial co-ordinates of markers. *J. Biomechanics* **13,** 391–393.

Woltring, H. J. (1990) Modeling and measurement errors in kinematics. In: Biomechanics of human movements—Applications in Ergonomics, Sports and Rehabilitation. *Proceedings of a Study Institute and Conference in Formia (Italy)* (Edited by Cappozzo, A. and Berme, N.) (in print).

Woltring, H. J. and Huiskes, R. (1985) A statistically motivated approach to instantaneous helical axis estimation from noisy, sampled landmark coordinates. In: *Biomechanics IX-B* (Edited by Winter, D. A., Norman, R. W., Wells, R. P., Hayes, K. C. and Patla, A. E.) pp. 274–279. Human Kinetics, Champaign, IL.

Woltring, H. J., Huiskes, R., Lange, A. de and Veldpaus, F. E. (1985) Finite centroid and helical axis estimation from noisy landmark measurements in the study of human joint kinematics. *J. Biomechanics* **18,** 379–389.